23

Continuum-Discrete Models for Supply Chains and Networks

Ciro D'Apice[1], Rosanna Manzo[1] and Benedetto Piccoli[2]
[1]*Department of Information Engineering and Applied Mathematics*
University of Salerno, Fisciano (SA)
[2]*Department of Mathematical Sciences, Rutgers University - Camden, Camden, NJ*
[1]*Italy*
[2]*United States*

1. Introduction

A supply network consists of suppliers, manufacturers, warehouses, and stores, that perform the functions of materials procurement, their transformation into intermediate and finished goods, and the distribution of the final products to customers among different production facilities. Mathematical models are used to monitor cost-efficient distribution of parts and to measure current business processes. The main aim is to plan supply networks so as to reduce the dead times and to avoid bottlenecks, obtaining as a result a greater coordination leading to the optimization of the production process of a given good. Several questions arise in the design of optimal supply chain networks: can we control the maximum processing rates, or the processing velocities, or the input flow in such way to minimize the value the queues attain and to achieve an expected outflow? The formulation of optimization problems for supply chain management is an immediate consequence of performing successful supply modeling and hence simulations.

Depending on the scale, supply networks modelling is characterized by different mathematical approaches: discrete event simulations and continuous models. Since discrete event models are based on considerations of individual parts, the principal drawback of them, however, is their enormous computational effort. A cost-effective alternative to discrete event models is continuous models (e.g. for models based on ordinary differential equations see Daganzo (2003), Helbing et al. (2004), Nagatani & Helbing (2004), Helbing & Lämmer (2005), Helbing et al. (2006)), in particular fluid-like network models using partial differential equations describing averaged quantities like density and average velocity (see Armbruster et al. (2004), Göttlich et al. (2005), Armbruster et al. (2006a), Armbruster et al. (2006b), Armbruster et al. (2006c), Göttlich et al. (2006), Herty et al. (2007), D'Apice et al. (2010)). Probably the first paper for supply chains in continuous direction was Armbruster et al. (2006b) where the authors, taking the limit on the number of parts and suppliers, have obtained a conservation law, whose flux is described by the minimum among the parts density and the maximal productive capacity.

Due to the difficulty of finding solution for the general equation proposed in Armbruster et al. (2006b), other fluid dynamic models for supply chains were introduced in Göttlich et al. (2005), D'Apice & Manzo (2006) and Bretti et al. (2007).

The work D'Apice & Manzo (2006) is based on a mixed continuum-discrete model, i.e. the supply chain is described by a graph consisting of consecutive arcs separated by nodes. The arcs represent processors or sub-chains, while the nodes model connections between arcs at which the dynamics can be regulated. The chain load, expressed by the part density and the processing rate, follows a time-space continuous evolution on arcs, and at nodes the conservation of the goods density is imposed, but not of the processing rate. In fact, on each arc an hyperbolic system of two equations is considered: a conservation law for the goods density, and a semi-linear evolution equation for the processing rate. At nodes a way to solve Riemann Problems, i.e. Cauchy problems with constant initial data on each arc, is prescribed and a solution at nodes guaranteeing the conservation of fluxes is defined. Moreover, existence of solutions to Cauchy problems was proved.
The paper Göttlich et al. (2005) deals with a conservation law, with constant processing rate, inside each supply sub-chain, with an entering queue for exceeding parts. The dynamics at a node is solved considering an ode for the queue. Some optimization technique for the model described in Göttlich et al. (2005) is developed in Göttlich et al. (2006), while the existence of solutions to Cauchy problems with the front tracking method is proved in Herty et al. (2007). In particular in Göttlich et al. (2006) the question of optimal operating velocities for each individual processing unit is treated for a supply chain network consisting of three processors. The maximal processing rates are fixed and not subject to change. The controls are the processing velocities. Given some default initial velocities the processing velocities are found to minimize the height of the buffering queues and producing a certain outflow. Moreover given a supply chain network with a vertex of dispersing type, the distribution rate has been controlled in such way to minimize the queues.
It is evident that the models described in Göttlich et al. (2005) and D'Apice & Manzo (2006) complete each other. In fact, the approach of Göttlich et al. (2005) is more suitable when the presence of queue with buffer is fundamental to manage goods production. The model of D'Apice & Manzo (2006), on the other hand, is useful when there is the possibility to reorganize the supply chain: in particular, the productive capacity can be readapted for some contingent necessity.
Starting from the model introduced in D'Apice & Manzo (2006) and fixing the rule that the objects are processed in order to maximize the flux, two different Riemann Solvers are defined and equilibria at a node are discussed in Bretti et al. (2007). Moreover, discretization algorithms to find approximated solution to the problem are described, numerical experiments on sample supply chains are reported and discussed for both the Riemann Solvers.
In D'Apice et al. (2010) existence of solutions to Cauchy problems is proven for both continuum-discrete supply chains and networks models, deriving estimates on the total variation of the density flux, density and processing rate along a wave-front tracking approximate solution.
Observe that while the papers Armbruster et al. (2006b), D'Apice & Manzo (2006), Bretti et al. (2007) treat the case of chains, i.e. sequential processors, modelled by a real line seen as a sequence of sub-chains corresponding to real intervals, the model in Göttlich et al. (2005) and the extended results in Göttlich et al. (2006), Herty et al. (2007), D'Apice et al. (2009) refer to networks.
In this Chapter we describe the continuum-discrete models for supply chains and networks reporting the main results of D'Apice & Manzo (2006), Bretti et al. (2007) and D'Apice et al. (2009).

We recall the basic supply chain model under consideration: a supply chain consists of sequential processors or arcs which are going to assemble and construct parts. Each processor is characterized by a maximum processing rate μ^e, its length L^e and the processing time T^e. The rate L^e/T^e represents the processing velocity.
The supply chain is modelled by a real line seen as a sequence of arcs corresponding to real intervals $[a^e, b^e]$ such that $[a^e, b^e] \cap [a^{e+1}, b^{e+1}] = v^e$: a node separating arcs. The dynamic of each arc is governed by a continuum system of the type

$$\rho_t + f_\varepsilon(\rho, \mu)_x = 0,$$

$$\mu_t - \mu_x = 0,$$

where $\rho(t,x) \in [0, \rho_{max}]$ is the density of objects processed by the supply chain at point x and time t and $\mu(t,x) \in [0, \mu_{max}]$ is the processing rate. For $\varepsilon > 0$, the flux f_ε is given by:

$$f_\varepsilon(\rho, \mu) = \begin{cases} m\rho, & \text{if } \rho \leq \mu, \\ m\mu + \varepsilon(\rho - \mu), & \text{if } \rho \geq \mu, \end{cases}$$

where m is the processing velocity.
The evolution at nodes v^e has been interpreted thinking to it as Riemann Problems for the density equation with μ data as parameters. Keeping the analogy to Riemann Problems, we call the latter Riemann Solver at nodes. In D'Apice & Manzo (2006) the following rule was used:

SC1 The incoming density flux is equal to the outgoing density flux. Then, if a solution with only waves in the density ρ exists, then such solution is taken, otherwise the minimal μ wave is produced.

Rule SC1 corresponds to the case in which processing rate adjustments are done only if necessary, while the density ρ can be regulated more freely. Thus, it is justified in all situations in which processing rate adjustments require re-building of the supply chain, while density adjustments are operated easily (e.g. by stocking). Even if rule SC1 is the most natural also from a geometric point of view, in the space of Riemann data, it produces waves only to lower the value of μ. As a consequence in some cases the value of the processing rate does not increase and it is not possible to maximize the flux. In order to avoid this problem two additional rules to solve dynamics at a node have been analyzed in Bretti et al. (2007):

SC2 The objects are processed in order to maximize the flux with the minimal value of the processing rate.

SC3 The objects are processed in order to maximize the flux. Then, if a solution with only waves in the density ρ exists, then such solution is taken, otherwise the minimal μ wave is produced.

The continuum-discrete model, regarding sequential supply chains, has been generalized to supply networks which consist of arcs and two types of nodes: nodes with one incoming arc and more outgoing ones and nodes with more incoming arcs and one outgoing arc.
The Riemann Problems are solved fixing two "routing" algorithms:

RA1 Goods from an incoming arc are sent to outgoing ones according to their final destination in order to maximize the flux over incoming arcs. Goods are processed ordered by arrival time (FIFO policy).

RA2 Goods are processed by arrival time (FIFO policy) and are sent to outgoing arcs in order to maximize the flux over incoming and outgoing arcs.

For both routing algorithms the flux of goods is maximized considering one of the two additional rules, SC2 and SC3.

In order to motivate the introduction of the model and to understand the mechanism of the above rules, we show some examples of real supply networks.

We analyze the behaviour of a supply network for assembling pear and apple fruit juice bottles, whose scheme is in Figure 1 (left).

Bottles coming from arc e^1 are sterilized in node v^1. Then, the sterilized bottles, with a certain probability α are directed to node v^3, where apple fruit juice is bottled, and with probability $1-\alpha$ to node 4, where the pear fruit juice is bottled. In nodes v^5 and v^6, bottles are labelled. Finally, in node 7, produced bottles are corked. Assume that pear and apple fruit juice bottles are produced using two different bottle shapes. The bottles are addressed from arc e^2 to the outgoing sub-chains e^3 and e^4 in which they are filled up with apple or pear fruit juice according to the bottle shape and thus according to their final destination: production of apple or pear fruit juice bottles. In a model able to describe this situation, the dynamics at node v^2 is solved using the RA1 algorithm. In fact, the redirection of bottles in order to maximize the production on both incoming and outgoing sub-chains is not possible, since bottles with apple and pear fruit juice have different shapes.

Consider a supply network for colored cups (Figure 1, right). The white cups are addressed towards n sub-chains in which they are colored using different colors. Since the aim is to maximize the cups production independently from the colors, a mechanism is realized which addresses the cups on the outgoing sub-chains by taking into account their loads in such way as to maximize flux on both incoming and outgoing sub-chains. It follows that a model realized to capture the behavior of the described supply network is based on rule RA2.

Let us now analyze an existing supply network where both algorithms shows up naturally: the chips production of the San Carlo enterprise. The productive processes follows various steps, that can be summarized in this way: when potatoes arrive at the enterprise, they are subjected to a goodness test. After this test, everything is ready for chips production, that starts with potatoes wash in drinking water. After washing potatoes, they are skinned off, rewashed and subjected to a qualification test. Then, they are cut by an automatic machine, and, finally, washed and dried by an air blow. At this point, potatoes are ready to be fried in vegetable oil for some minutes and, after this, the surplus oil is dripped. Potatoes are then salted by a dispenser, that nebulizes salt spreading it on potatoes. An opportune chooser

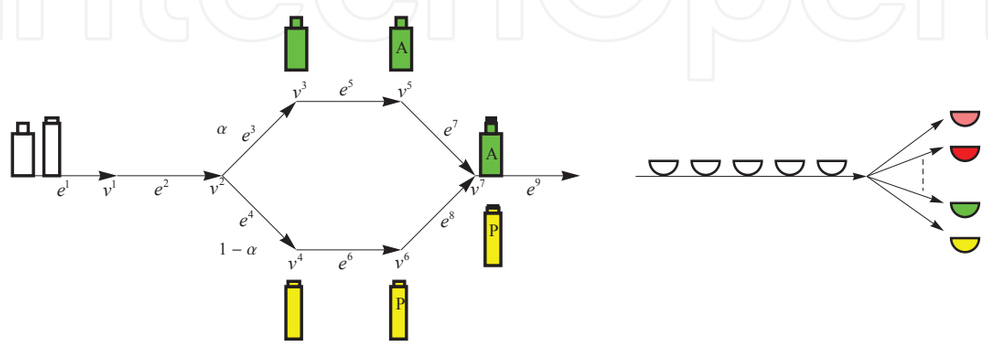

Fig. 1. Fruit juice network and cups production.

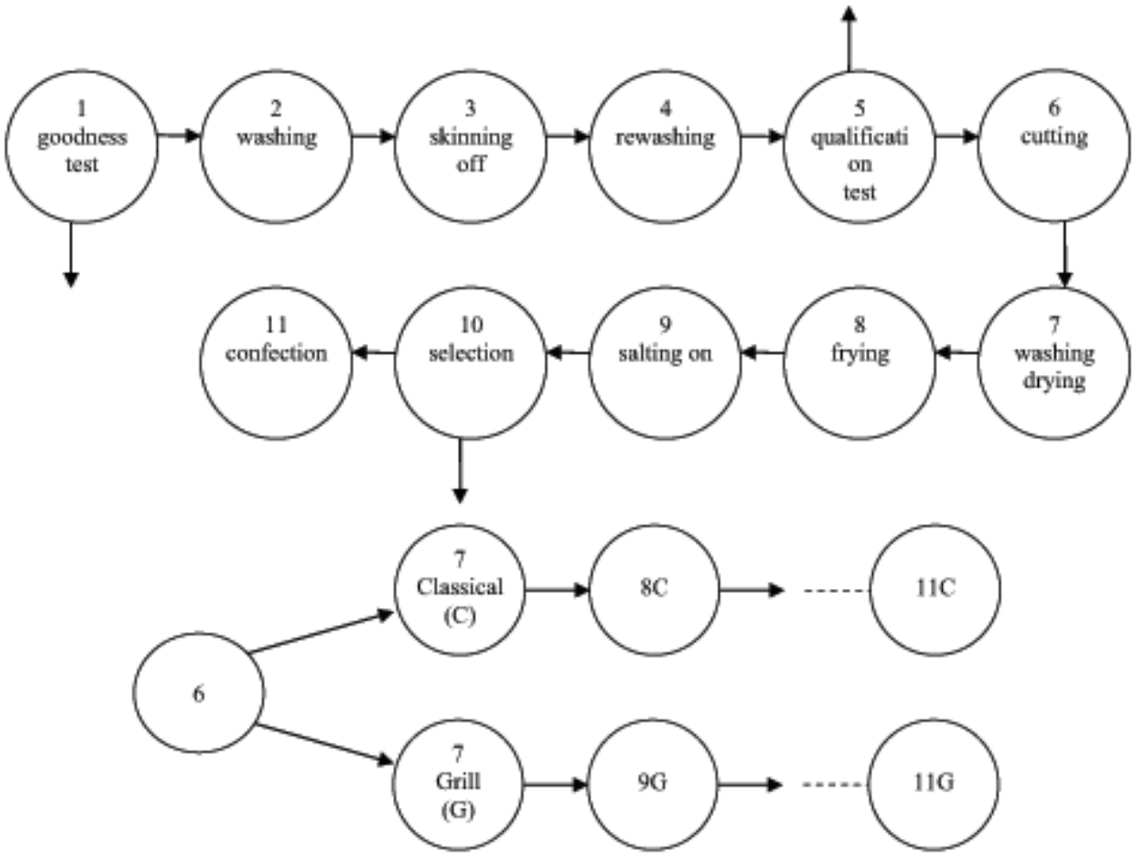

Fig. 2. Graph of the supply network for chips production (top) and possible arcs (bottom).

is useful to select the best products. The final phase of the process is given by potatoes confection. A simplified vision of the supply chain network is in Fig. 2 (top).

In phases 1, 5 and 10 a discrimination is made in production in order to distinguish good and bad products. In such sense, we can say that there is a statistical percentage α of product, that follows the production steps, while the percentage $1-\alpha$ is the product discarded (obviously, the percentage α can be different for different phases). Therefore, the goods routing in these nodes follows the algorithm RA1. On the other side, phase 6 concerns the potatoes cut: as the enterprise produces different types of fried potatoes (classical, grill, light, stick, etc.), different ways of cutting potatoes must be considered. Assume that, for simplicity, there are only two types of potatoes production, then the supply network is as in Fig. 2 (bottom). If the aim is only the production maximization independently from the type, then the potatoes are addressed from node 6 towards the outgoing arcs according to the RA2 algorithm.

The Chapter is organized as follows. Section 2 is devoted the description of the continuum-discrete model for supply chain. In particular Subsection 2.1 gives the basic definitions of supply chain and Riemann Solver. Then the dynamics inside an arc is studied. In Subsection 2.2 particular Riemann Solvers according to rules SC1, SC2 and SC3 are defined and explicit unique solutions are given. Moreover test simulations are reported. Section 3 extends the model to simple supply networks.

2. A continuum-discrete model for supply chains

In this Section we present a model able to describe the load dynamics on supply chains, i.e. sequential processors, modelled by a real line seen as a sequence of sub-chains corresponding to real intervals.

2.1 Basic definitions

We start from the conservation law model of Armbruster et al. (2006b):

$$\rho_t + (\min\{\mu(t,x),\rho\})_x = 0. \tag{1}$$

To avoid problems of existence of solutions, we assume μ piecewise constant and an evolution equation of semi-linear type:

$$\mu_t + \overline{V}\mu_x = 0, \tag{2}$$

where $\overline{V}$ is some constant velocity. Taking $\overline{V} = 0$, we may have no solution to a Riemann Problem for the system (1)–(2) with data (ρ_l,μ_l) and (ρ_r,μ_r) if $\min\{\mu_l,\rho_l\} > \mu_r$. Since we expect the chain to influence backward the processing rate we assume $\overline{V} < 0$ and for simplicity we set $\overline{V} = -1$.

We define a mixed continuum-discrete model in the following way. On each arc e, the evolution is given by (1)–(2). On the other side, the evolution at nodes v^e is given solving Riemann Problems for the density equation (1) with μs as parameters. Such Riemann Problems may still admit no solution as before if we keep the values of the parameters μs constant, thus we expect μ waves to be generated and then follow equation (2). The vanishing of the characteristic velocity for (1), in case $\rho > \mu$, can provoke resonances with the nodes (which can be thought as waves with zero velocities). Therefore, we slightly modify the model as follows.

Each arc e is characterized by a maximum density $\rho^e_{\max}$, a maximum processing rate $\mu^e_{\max}$ and a flux f^e_ε. For a fixed $\varepsilon > 0$, the dynamics is given by:

$$\begin{cases} \rho_t + f^e_\varepsilon(\rho,\mu)_x = 0, \\ \mu_t - \mu_x = 0. \end{cases} \tag{3}$$

The flux is defined as:

(F) $$f^e_\varepsilon(\rho,\mu) = \begin{cases} \rho, & 0 \le \rho \le \mu, \\ \mu + \varepsilon(\rho-\mu), & \mu \le \rho \le \rho^e_{\max}, \end{cases}$$

$$f^e_\varepsilon(\rho,\mu) = \begin{cases} \varepsilon\rho + (1-\varepsilon)\mu, & 0 \le \mu \le \rho, \\ \rho, & \rho \le \mu \le \mu^e_{\max}, \end{cases}$$

see Figure 3.

The conservation law for the good density in (3) is a ε perturbation of (1) in the sense that $\|f - f_\varepsilon\|_\infty \le C\varepsilon$, where f is the flux of (1). The equation has the advantage of producing waves with always strictly positive speed, thus avoiding resonance with the "boundary"problems at nodes v^e.

Remark 1 *We can consider a slope m, defining the flux*

$$f_\varepsilon(\rho,\mu) = \begin{cases} m\rho, & \text{if } \rho \le \mu, \\ m\mu + \varepsilon(\rho-\mu), & \text{if } \rho \ge \mu, \end{cases} \tag{4}$$

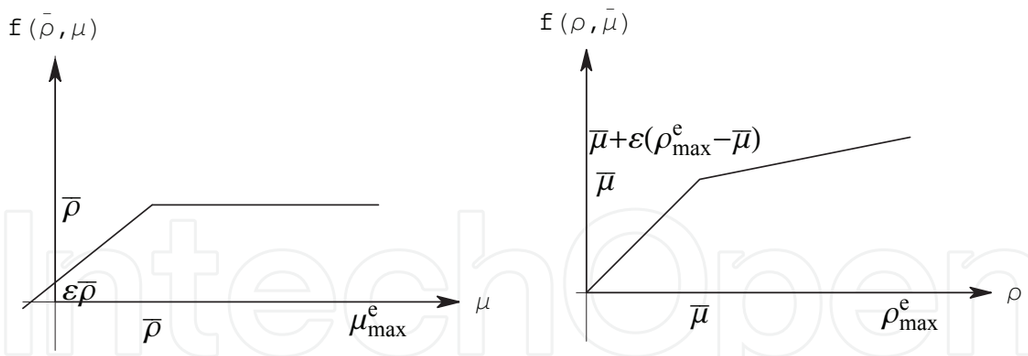

Fig. 3. Flux (F): Left, $f(\bar{\rho},\mu)$. Right, $f(\rho,\bar{\mu})$.

or different slopes m^e, considering the flux

$$f^e_\varepsilon(\rho,\mu)=\begin{cases} m^e\rho, & 0\le\rho\le\mu,\\ m^e\mu+\varepsilon(\rho-\mu), & \mu\le\rho\le\rho^e_{\max}, \end{cases} \tag{5}$$

where $m^e\ge 0$ represents the velocity of each processor and is given by $m^e=\frac{L^e}{T^e}$, with L^e and T^e, respectively, fixed length and processing time of processor e.

From now on, for simplicity we assume that ε is fixed and the flux is the same for each arc e, we then drop the indices thus indicate the flux by $f(\rho,\mu)$. The general case can be treated similarly.
The supply chain evolution is described by a finite set of functions ρ^e,μ^e defined on $[0,+\infty[\times[a^e,b^e]$. On each sub-chain $[a^e,b^e]$, we say that $U^e:=(\rho^e,\mu^e):[0,+\infty[\times[a^e,b^e]\ \mapsto\mathbb{R}$ is a weak solution to (3) if, for every C^∞-function $\varphi:[0,+\infty[\times[a^e,b^e]\ \mapsto\mathbb{R}^2$ with compact support in $]0,+\infty[\times\,]a^e,b^e[$,

$$\int_0^{+\infty}\int_{a^e}^{b^e}\left(U^e\cdot\frac{\partial\varphi}{\partial t}+f(U^e)\cdot\frac{\partial\varphi}{\partial x}\right)dx\,dt=0,$$

where

$$f(U^e)=\begin{pmatrix} f(\rho^e,\mu^e)\\ -\mu^e\end{pmatrix},$$

is the flux function of the system (3). For the definition of entropy solution, we refer to Bressan (2000).
For a scalar conservation law, a Riemann Problem (RP) is a Cauchy problem for an initial data of Heavyside type, that is piecewise constant with only one discontinuity. One looks for centered solutions, i.e. $\rho(t,x)=\phi(\frac{x}{t})$ formed by simple waves, which are the building blocks to construct solutions to the Cauchy problem via wave- front tracking algorithm. These solutions are formed by continuous waves called rarefactions and by travelling discontinuities called shocks. The speed of waves are related to the values of f', see Bressan (2000).
Analogously, we call Riemann Problem for a junction the Cauchy problem corresponding to an initial data which is constant on each supply line.

Definition 2 *A Riemann Solver for the node v^e consists in a map RS : $[0,\rho^e_{\max}]\times[0,\mu^e_{\max}]\times[0,\rho^{e+1}_{\max}]\times[0,\mu^{e+1}_{\max}]\ \mapsto\ [0,\rho^e_{\max}]\times[0,\mu^e_{\max}]\times[0,\rho^{e+1}_{\max}]\times[0,\mu^{e+1}_{\max}]$ that associates to a Riemann data $(\rho^{e,0},\mu^{e,0},\rho^{e+1,0},\mu^{e+1,0})$ at v^e a vector*

$(\hat{\rho}^e, \hat{\mu}^e, \hat{\rho}^{e+1}, \hat{\mu}^{e+1})$ so that the solution is given by the waves $(\rho^{e,0}, \hat{\rho}^e)$ and $(\mu^{e,0}, \hat{\mu}^e)$ on the arc e and by the waves $(\hat{\rho}^{e+1}, \rho^{e+1,0})$, and $(\hat{\mu}^{e+1}, \mu^{e+1,0})$ on the arc $e+1$. We require the consistency condition

(CC) $RS(RS(\rho^{e,0}, \mu^{e,0}, \rho^{e+1,0}, \mu^{e+1,0})) = RS((\rho^{e,0}, \mu^{e,0}, \rho^{e+1,0}, \mu^{e+1,0}))$.

Once a Riemann Solver is assigned we can define admissible solutions at v^e.

Definition 3 *Assume a Riemann Solver RS is assigned for the node v^e. Let $U = (U^e, U^{e+1})$ be such that $U^e(t,\cdot)$ and $U^{e+1}(t,\cdot)$ are of bounded variation for every $t \geq 0$. Then U is an admissible weak solution of (3) related to RS at the junction v^e if and only if the following property holds for almost every t. Setting*

$$\widetilde{U}^e(t) = (U^e(\cdot, b^e-), U^{e+1}(\cdot, a^e+))$$

we have $RS(\widetilde{U}^e(t)) = \widetilde{U}^e(t)$.

Our aim is to solve the Cauchy problem for $t \geq 0$ for given initial data.

2.1.1 Dynamics on arcs

Let us fix an arc e and analyze system (3): it is a system of conservation laws in the variables $U = (\rho, \mu)$:

$$U_t + F(U)_x = 0, \tag{6}$$

with flux function given by $F(U) = (f(\rho,\mu), -\mu)$, thus the Jacobian matrix of the flux is:

$$DF(\rho,\mu) = \begin{cases} \begin{pmatrix} 1 & 0 \\ 0 & -1 \end{pmatrix}, & \text{if } \rho < \mu, \\ \\ \begin{pmatrix} \varepsilon & 1-\varepsilon \\ 0 & -1 \end{pmatrix}, & \text{if } \rho > \mu. \end{cases}$$

The eigenvalues and eigenvectors are given by:

$$\lambda_1(\rho,\mu) = -1, \qquad r_1(\rho,\mu) = \begin{cases} \begin{pmatrix} 0 \\ 1 \end{pmatrix}, & \text{if } \rho < \mu, \\ \\ \begin{pmatrix} -\frac{1-\varepsilon}{1+\varepsilon} \\ 1 \end{pmatrix}, & \text{if } \rho > \mu, \end{cases}$$

$$\lambda_2(\rho,\mu) = \begin{cases} 1, & \text{if } \rho < \mu, \\ \varepsilon, & \text{if } \rho > \mu, \end{cases} \qquad r_2(\rho,\mu) = \begin{pmatrix} 1 \\ 0 \end{pmatrix}.$$

Hence the Hugoniot curves for the first family are vertical lines above the secant $\rho = \mu$ and lines with slope close to $-1/2$ below the same secant. The Hugoniot curves for the second family are just horizontal lines. Since we consider positive and bounded values for the variables, we fix the invariant region:

$$\mathcal{D} = \{(\rho,\mu) : 0 \leq \rho \leq \rho_{max},\ 0 \leq \mu \leq \mu_{max},$$

$$0 \leq (1+\varepsilon)\rho + (1-\varepsilon)\mu \leq (1+\varepsilon)\rho_{max} = 2(1-\varepsilon)\mu_{max}\}$$

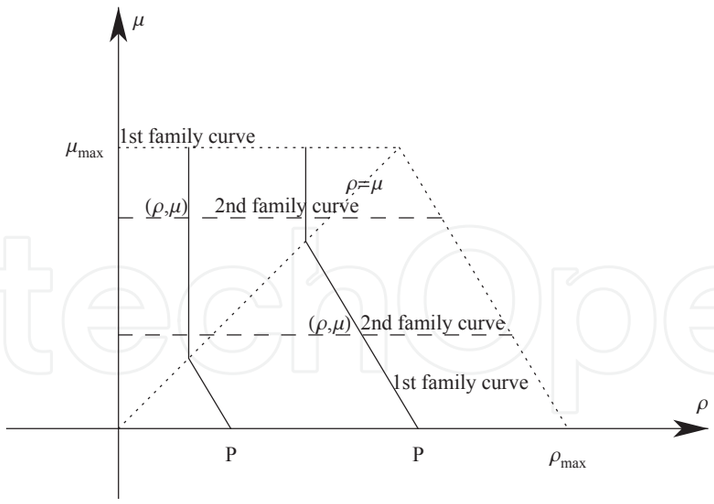

Fig. 4. First and second family curves.

see Figure 4.
Observe that

$$\rho_{\max} = \mu_{\max} \frac{2}{1+\varepsilon}. \tag{7}$$

Proposition 4 *Given (ρ^0, μ^0), the minimal value of the flux at points of the curve of the first family passing through (ρ^0, μ^0) is given by:*

$$f_{min}((\rho^0, \mu^0)) = \begin{cases} \frac{2\varepsilon}{1+\varepsilon}\rho^0, & if\ \rho^0 \leq \mu^0, \\ \varepsilon\rho^0 + \frac{\varepsilon(1-\varepsilon)}{1+\varepsilon}\mu^0, & if\ \rho^0 > \mu^0. \end{cases}$$

Lemma 5 *Given an initial datum (ρ^0, μ^0), the maximum value of the density of the curve of the second family passing through (ρ^0, μ^0) and belonging to the invariant region is given by*

$$\rho_M(\mu^0) = \rho_{\max} - \mu^0 \frac{\rho_{\max} - \mu_{\max}}{\mu_{\max}}. \tag{8}$$

2.2 Riemann Solvers at nodes

In this Section we discuss possible definitions of a general Riemann Solver, which conserves the flux at nodes. We fix a node v^e and a Riemann initial datum: constantly equal to $(\rho^{e,0}, \mu^{e,0})$ on e and constantly equal to $(\rho^{e+1,0}, \mu^{e+1,0})$ on $e+1$.
First observe that the following Lemmas hold:

Lemma 6 *On the incoming arc, only waves of the first family may be produced, while on the outgoing arc only waves of the second family may be produced.*

Lemma 7 *The Riemann Problem at node v^e admits a solution if the following holds.*
If $\rho^{e,0} \leq \mu^{e,0}$ then

$$\mu^{e+1,0}(1-\varepsilon) + \varepsilon(\rho^{e+1}_{\max} - \frac{2}{1+\varepsilon}\rho^{e,0}) \geq 0. \tag{9}$$

If $\rho^{e,0} > \mu^{e,0}$ *then*

$$(1-\varepsilon)\left(\mu^{e+1,0} - \frac{\varepsilon}{1+\varepsilon}\mu^{e,0}\right) + \varepsilon(\rho^{e+1}_{\max} - \rho^{e,0}) \geq 0. \tag{10}$$

Remark 8 *Conditions (9) and (10) are fulfilled if* $\rho^{e+1}_{\max} \geq 2\rho^{e,0}$ *and* $\mu^{e+1,0} \geq \mu^{e,0}$*, which is a condition on the initial datum.*

We are now ready to describe a general solution to a Riemann Problem at v^e. From Lemma 6, given the initial datum $(\rho^{e,0}, \mu^{e,0}, \rho^{e+1,0}, \mu^{e+1,0})$, for every Riemann Solver it follows that

$$\hat{\rho}^e = \varphi(\hat{\mu}^e),$$

$$\hat{\mu}^{e+1} = \mu^{e+1,0},$$

where the function $\varphi(\cdot)$ describes the first family curve through $(\rho^{e,0}, \mu^{e,0})$ as function of $\hat{\mu}^e$:

$$\varphi(\hat{\mu}^e) = \begin{cases} \bar{\mu}^e, & \text{if } \hat{\mu}^e \geq \bar{\mu}^e, \\ \frac{(\varepsilon-1)\hat{\mu}^e + 2\rho^{e,0}}{1+\varepsilon}, & \text{if } \hat{\mu}^e < \bar{\mu}^e, \rho^{e,0} \leq \mu^{e,0}, \\ \frac{(\varepsilon-1)(\hat{\mu}^e - \mu^{e,0}) + (1+\varepsilon)\rho^{e,0}}{1+\varepsilon}, & \text{if } \hat{\mu}^e < \bar{\mu}^e, \rho^{e,0} > \mu^{e,0}, \end{cases}$$

with $\bar{\mu}^e$ the value in which the expression of such curve changes:

$$\bar{\mu}^e = \begin{cases} \rho^{e,0}, & \text{if } \rho^{e,0} \leq \mu^{e,0}, \\ \frac{1+\varepsilon}{2}\rho^{e,0} + \frac{1-\varepsilon}{2}\mu^{e,0}, & \text{if } \rho^{e,0} > \mu^{e,0}. \end{cases} \tag{11}$$

Let us now discuss how $\hat{\rho}^{e+1}$ and $\hat{\mu}^e$ can be chosen. The conservation of flux at the node can be written as

$$f(\varphi(\hat{\mu}^e), \hat{\mu}^e) = f(\hat{\rho}^{e+1}, \mu^{e+1,0}). \tag{12}$$

We have to distinguish two cases:

Case α) $\mu^{e+1,0} < \bar{\mu}^e$;

Case β) $\bar{\mu}^e \leq \mu^{e+1,0}$.

In both cases $\bar{\mu}^e$ and $\mu^{e+1,0}$ individuate in the plane $(\hat{\rho}^{e+1}, \hat{\mu}^e)$ four regions, A, B, C, D, so defined:

$$\begin{aligned} A &= \{(\hat{\rho}^{e+1}, \hat{\mu}^e) : 0 \leq \hat{\rho}^{e+1} \leq \mu^{e+1,0}, \bar{\mu}^e \leq \hat{\mu}^e \leq \mu^e_{\max}\}; \\ B &= \{(\hat{\rho}^{e+1}, \hat{\mu}^e) : \mu^{e+1,0} \leq \hat{\rho}^{e+1} \leq \rho^{e+1}_{\max}, \bar{\mu}^e \leq \hat{\mu}^e \leq \mu^e_{\max}\}; \\ C &= \{(\hat{\rho}^{e+1}, \hat{\mu}^e) : 0 \leq \hat{\rho}^{e+1} \leq \mu^{e+1,0}, 0 \leq \hat{\mu}^e \leq \bar{\mu}^e\}; \\ D &= \{(\hat{\rho}^{e+1}, \hat{\mu}^e) : \mu^{e+1,0} \leq \hat{\rho}^{e+1} \leq \rho^{e+1}_{\max}, 0 \leq \hat{\mu}^e \leq \bar{\mu}^e\}. \end{aligned}$$

The equation (12) is satisfied in case β) along the line depicted in Figure 5 and in case α) there are solutions, only under some conditions, along the dashed line.

2.2.1 A Riemann Solver according to rule SC1.

A geometrically natural Riemann Solver is the following. In case β) we can define a Riemann Solver mapping every initial datum on the line $\hat{\mu}^e = c$ to the intersection of the same line with that drawn in Figure 5.
In case α), it may happen that there is no admissible solution on a given line $\hat{\mu}^e = c$. Therefore, we can use the same procedure if the line $\hat{\mu}^e = c$ intersects the dashed line of Figure 5, while mapping all other points to the admissible solution with the highest value of $\hat{\mu}^e$.
The obtained Riemann Solver is depicted in Figure 6 and satisfies the policy SC1. On the left, there is case β) with all points mapped horizontally, while, on the right, there is case α): all points of the white region are mapped horizontally and all points of the dark region are mapped to the point indicated by the arrow.

Remark 9 *If $\hat{\rho}^{e+1} \leq \mu^{e+1,0}$, then the solution $(\hat{\rho}^{e+1}, \rho^{e+1,0})$ is a contact discontinuity. The same happens if $\hat{\rho}^{e+1} \geq \mu^{e+1,0}$ and $\hat{\rho}^{e+1} > \mu^{e+1,0}$. If $\hat{\rho}^{e+1} > \mu^{e+1,0}$ and $\rho^{e+1,0} < \mu^{e+1,0}$, the solution consists of two contact discontinuities.*

Let us define in detail the Riemann Solver described in Figure 6. We introduce the notations:

$$f^e_{\max} = f(\rho^e_{\max}, \mu^{e,0}),$$

$$f^{e+1}_{\max} = f(\rho^{e+1}_{\max}, \mu^{e+1,0}).$$

Proposition 10 *Fix a node v^e. For every Riemann initial datum $(\rho^{e,0}, \mu^{e,0}, \rho^{e+1,0}, \mu^{e+1,0})$ at v^e there exists a unique vector $(\hat{\rho}^e, \hat{\mu}^e, \hat{\rho}^{e+1}, \hat{\mu}^{e+1})$ such that:*

a) if $f(\rho^{e,0}, \mu^{e,0}) \leq f^{e+1}_{\max}$, then

$$\hat{\mu}^e = \mu^{e,0}, \quad \hat{\mu}^{e+1} = \mu^{e+1,0},$$

$$\hat{\rho}^e = \rho^{e,0},$$

$$\hat{\rho}^{e+1} = \begin{cases} f(\rho^{e,0}, \mu^{e,0}), & \text{if } f(\rho^{e,0}, \mu^{e,0}) \leq \mu^{e+1,0}, \\ \frac{f(\rho^{e,0}, \mu^{e,0}) - \mu^{e+1,0}}{\varepsilon} + \mu^{e+1,0}, & \text{if } \mu^{e+1,0} \leq f(\rho^{e,0}, \mu^{e,0}) \leq f^{e+1}_{\max}, \end{cases}$$

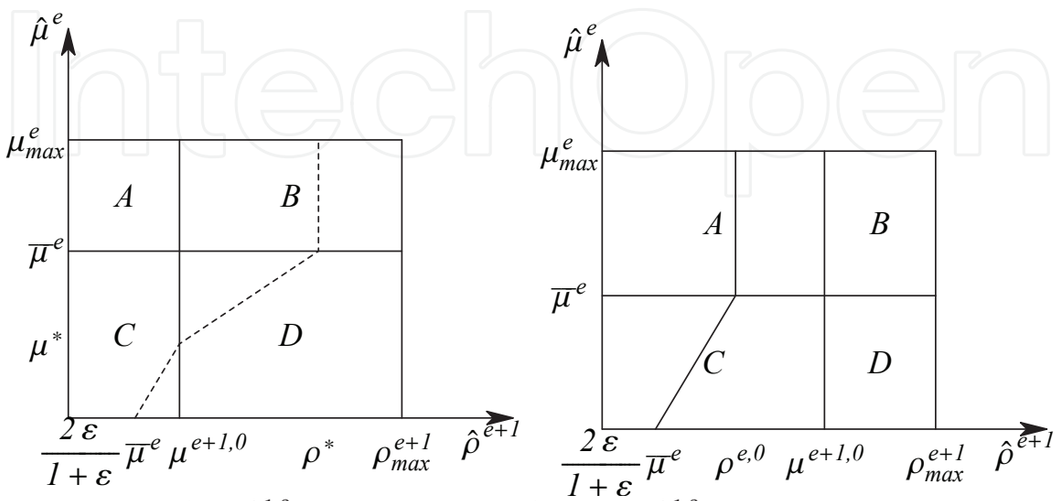

Fig. 5. Left: Case α) : $\mu^{e+1,0} < \bar{\mu}^e$. Right: Case β) : $\bar{\mu}^e \leq \mu^{e+1,0}$.

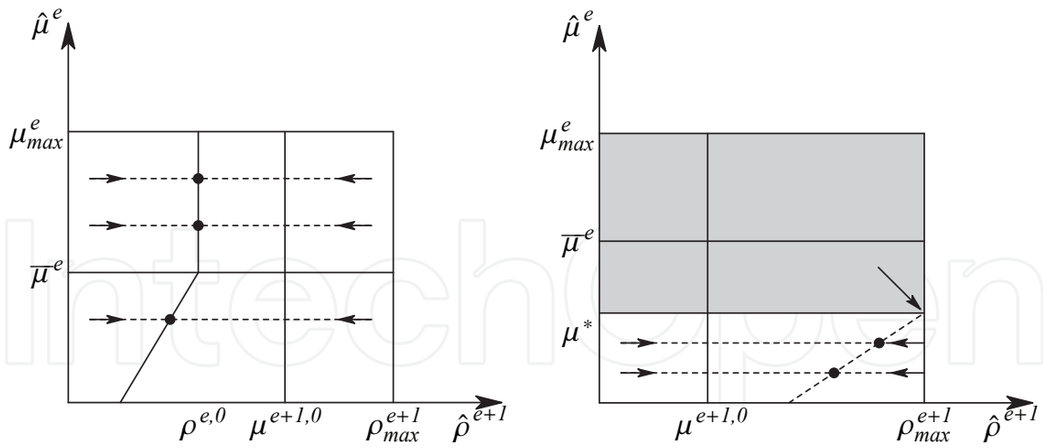

Fig. 6. An example of Riemann Solver: case β) (on the left) and α) (on the right).

b) if $f(\rho^{e,0},\mu^{e,0}) > f^{e+1}_{\max}$, *then*

$$\hat{\rho}^e = \rho^{e,0}, \quad \hat{\rho}^{e+1} = \rho^{e+1}_{\max},$$
$$\hat{\mu}^e = \frac{f^{e+1}_{\max} - \varepsilon\rho^{e,0}}{1-\varepsilon}, \quad \hat{\mu}^{e+1} = \mu^{e+1,0}.$$

Theorem 11 *The Riemann Solver described in Proposition 10 is in accordance to rule SC1.*

Let us pass now to consider solvability of Riemann Problems according to the Riemann Solver above.

Lemma 12 *Consider a supply chain on which the initial datum verifies* $\mu^{e,0} = \mu^e_{\max}$, *i.e. the production rate is at its maximum. A sufficient condition for the solvability of all Riemann Problems, according to rule SC1, on the supply chain at every time is*

$$\rho^{e+2}_{\max} \geq \rho^e_{\max}, \forall e.$$

2.2.2 A Riemann Solver according to rule SC2.

Rule SC2 individuates a unique Riemann Solver as shown by next:

Theorem 13 *Fix a node* v^e. *For every Riemann initial datum* $(\rho^{e,0}, \mu^{e,0}, \rho^{e+1,0}, \mu^{e+1,0})$ *at* v^e *there exists a unique vector* $(\hat{\rho}^e, \hat{\mu}^e, \hat{\rho}^{e+1}, \hat{\mu}^{e+1})$ *solution of the Riemann Problem according to rule SC2.*

Case α) $\mu^{e+1,0} < \bar{\mu}^e$

Case α_1) $\rho^* \leq \rho_M(\mu^{e+1,0})$

$$\hat{\rho}^e = \varphi(\hat{\mu}^e), \quad \hat{\mu}^e = \min\{\mu^e_{\max}, \rho^*\},$$
$$\hat{\rho}^{e+1} = \rho^*, \quad \hat{\mu}^{e+1} = \mu^{e+1,0},$$

Case α_2) $\rho^* > \rho_M(\mu^{e+1,0})$

$$\hat{\rho}^e = \varphi(\hat{\mu}^e), \quad \hat{\mu}^e = \tilde{\mu},$$
$$\hat{\rho}^{e+1} = \rho_M(\mu^{e+1,0}), \quad \hat{\mu}^{e+1} = \mu^{e+1,0},$$

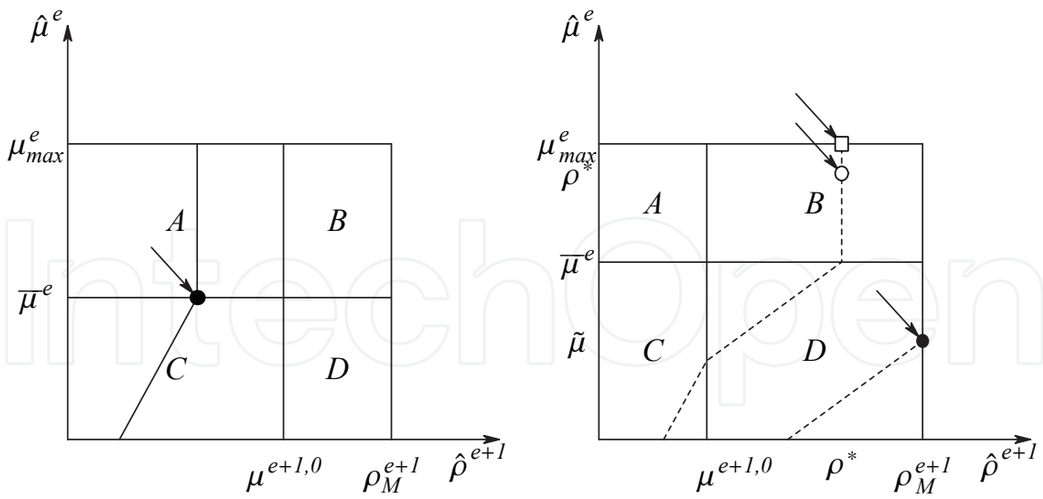

Fig. 7. Case β) (on the left) and α) (on the right) for the Riemann solver SC2.

Case β) $\mu^{e+1,0} \geq \bar{\mu}^e$

$$\hat{\rho}^e = \varphi(\hat{\mu}^e), \quad \hat{\mu}^e = \bar{\mu}^e,$$
$$\hat{\rho}^{e+1} = \bar{\mu}^e, \quad \hat{\mu}^{e+1} = \mu^{e+1,0},$$

where $\rho^* = \frac{\bar{\mu}^e - (1-\varepsilon)\mu^{e+1,0}}{\varepsilon}$, *and* $\tilde{\mu} = \frac{2\varepsilon}{1-\varepsilon}(\mu^e_{\max} - \bar{\mu}^e) + \mu^{e+1,0}$.

This Riemann Solver is depicted in Figure 7. In case β) we can define a Riemann Solver mapping every initial datum to the point $(\bar{\mu}^e, \bar{\mu}^e)$, indicated by the arrow.
In case α), we can define a Riemann Solver mapping every initial datum to the circle or to the square point if $\rho^* \leq \rho_M$ and to the filled point if $\rho^* > \rho_M$.

2.2.3 A Riemann Solver according to rule SC3.

Also rule SC3 determines a unique Riemann Solver as shown by next:

Theorem 14 *Fix a node* v^e. *For every Riemann initial datum* $(\rho^{e,0}, \mu^{e,0}, \rho^{e+1,0}, \mu^{e+1,0})$ *at* v^e *there exists a unique vector* $(\hat{\rho}^e, \hat{\mu}^e, \hat{\rho}^{e+1}, \hat{\mu}^{e+1})$ *solution of the Riemann Problem according to rule SC3.*

Case α) $\mu^{e+1,0} < \bar{\mu}^e$

Case α_1) $\rho^* \leq \rho_M(\mu^{e+1,0})$

Case $\alpha_{1.1}$) $\rho^* > \mu^e_{\max}$

$$\hat{\rho}^e = \varphi(\hat{\mu}^e), \quad \hat{\mu}^e = \mu^e_{\max},$$
$$\hat{\rho}^{e+1} = \rho^*, \quad \hat{\mu}^{e+1} = \mu^{e+1,0},$$

Case $\alpha_{1.2}$) $\rho^* \leq \mu^e_{\max}$

$$\hat{\rho}^e = \varphi(\hat{\mu}^e), \quad \hat{\mu}^e = \max\{\rho^*, \mu^{e,0}\},$$
$$\hat{\rho}^{e+1} = \rho^*, \quad \hat{\mu}^{e+1} = \mu^{e+1,0},$$

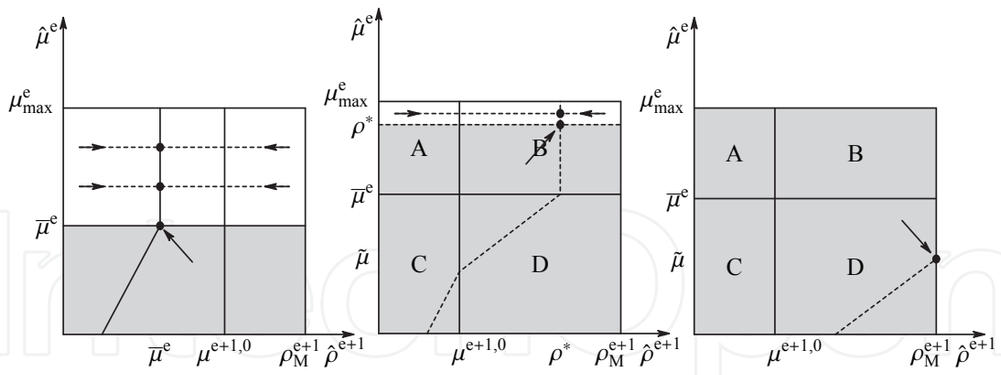

Fig. 8. Case β) and α) (namely α_1) and α_2)) for the Riemann Solver SC3.

Case α_2) $\quad \rho^* > \rho_M(\mu^{e+1,0})$

$$\hat{\rho}^e = \varphi(\hat{\mu}^e), \quad \hat{\mu}^e = \tilde{\mu},$$
$$\hat{\rho}^{e+1} = \rho_M(\mu^{e+1,0}), \quad \hat{\mu}^{e+1} = \mu^{e+1,0},$$

Case β) $\quad \mu^{e+1,0} \geq \bar{\mu}^e$

$$\hat{\rho}^e = \varphi(\hat{\mu}^e), \quad \hat{\mu}^e = \begin{cases} \bar{\mu}^e, & \text{if } \mu^{e,0} < \bar{\mu}^e, \\ \mu^{e,0}, & \text{if } \mu^{e,0} \geq \bar{\mu}^e, \end{cases}$$
$$\hat{\rho}^{e+1} = \bar{\mu}^e, \quad \hat{\mu}^{e+1} = \mu^{e+1,0},$$

where $\rho^* = \frac{\bar{\mu}^e - (1-\varepsilon)\mu^{e+1,0}}{\varepsilon}$, *and* $\tilde{\mu} = \frac{2\varepsilon}{1-\varepsilon}(\mu^e_{\max} - \bar{\mu}^e) + \mu^{e+1,0}$.

The obtained Riemann Solver is depicted in Figure 8: all points of the white region are mapped horizontally and all points of the dark regions are mapped to the point indicated by the arrows.
Analogously to the case of rule SC1, we can give conditions for solvability of Riemann Problems, more precisely:

Lemma 15 *Consider a supply chain on which the initial datum verifies* $\mu^{e,0} = \mu^e_{\max}$, *i.e. the production rate is at its maximum. A sufficient condition for the solvability of all Riemann Problems, according to rule SC2 or SC3, on the supply chain at every time is*

$$\rho^{e+2}_{\max} \geq \rho^e_{\max}, \forall e.$$

2.3 Numerical tests

As an application of the supply chain dynamics we present some experiments on sample cases. The problem (3) is discretized using Godunov and Upwind schemes. We set space increment equal on each arc, namely $N^e = \frac{L^e}{\Delta x}$, where N^e is the number of space discretization points. The time steps Δt are constants and are obtained imposing the CFL condition on each arc.
In the following Tests 1 and 2 we refer to numerical examples presented in Göttlich et al. (2005; 2006) in such a way to establish a comparison between their and our approach. To this aim we consider the flux function with different slopes (5).
Test 1. As in Göttlich et al. (2005), we analyze a supply chain network consisting of $N = 4$ arcs and we use the data in Table 1.

Processor e	μ^e	m^e	L^e
1	25	1	1
2	15	0.2	0.2
3	10	0.2	0.6
4	15	0.2	0.2

Table 1. Parameters of the test problem 1.

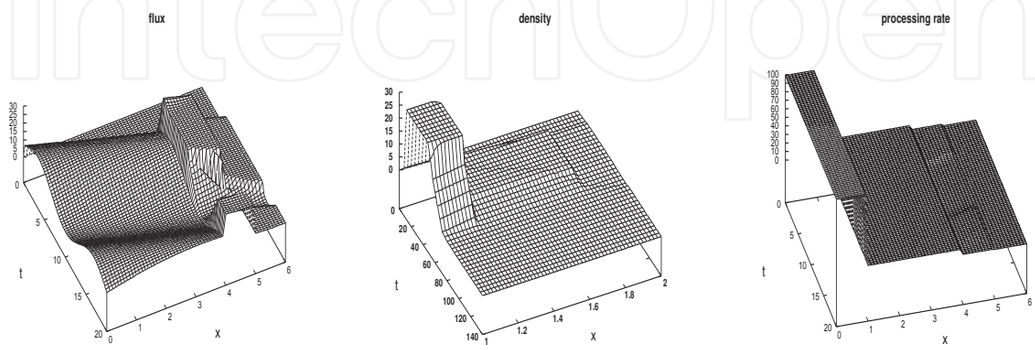

Fig. 9. Test 1: evolution on processors 2, 3, 4, of f (left), ρ (central) and μ (right) using SC1, with data in Table 1 and $\varepsilon = 0.1$.

Let us assume the following initial and boundary data:

$$\rho^1(0,x) = \rho^2(0,x) = \rho^3(0,x) = \rho^4(0,x) = 0,$$

$$\rho^1(t,0) = \begin{cases} \frac{18}{35}t, & 0 \le t \le 35, \\ -\frac{18}{35}t + 36, & 35 < t \le 70, \\ 0, & t > 70, \end{cases}$$

and the space and time intervals are, respectively, $[0,2]$ and $[0,140]$, with $\Delta x = 0.02$ and $\Delta t = 0.01$. On each processor $e = 1,2,3,4$ we assume as the initial datum $\mu(0,x)$ the value μ^e, which is also imposed at the incoming and outgoing boundaries. Notice that the inflow profile $\rho^1(t,0)$ is assigned on the first processor, which can be considered as an artificial arc, and it exceeds the maximum capacity of the other processors. In Fig. 9 it is depicted the evolution in time on processors 2, 3, 4, of flux, density and processing rate, obtained by the Riemann Solver SC1 for $\varepsilon = 0.1$. From the analysis of graphics in Fig. 9, we can deduce that the processing rate, according to SC1, is minimized and, consequently, the flux and the density are considerably lowered and are almost plateau shaped on processors 3 and 4. On the other hand, SC2 determines the behaviour showed in Fig. 10, where the flux and the density are correctly developed on processors 2, 3, 4, due to the behaviour of the processing rate depicted in the graphics, which assumes the minimum possible value in order to maximize the flux.
In the following Figg. 11, 12 and 13 it is depicted the evolution in time on processors 2, 3, 4, of flux, density and processing rate, as obtained by the Riemann Solver SC3 with, respectively, $\varepsilon = 0.1$, $\varepsilon = 0.5$ and $\varepsilon = 0.01$.
As showed by the graphics obtained, ε varying determines a different evolution. In particular, for ε tending to zero, the maximum values assumed by the flux and the density decrease.

Processor e	μ^e	L^e
1	99	1
2	15	1
3	10	3
4	8	1

Table 2. Parameters of the test problem 2.

From the analysis of graphics in Figg. 11, 12 and 13, obtained by applying Riemann Solver SC3, we can deduce that adjustments of processing rate determine the expected behaviour of the density, also in accordance with results reported in Göttlich et al. (2005).

Test 2.

Referring to Göttlich et al. (2006), we consider again a supply chain of $N = 4$ arcs and impose the following initial and boundary data:

$$\rho^1(0,x) = \rho^2(0,x) = \rho^3(0,x) = \rho^4(0,x) = 0,$$

$$\rho^1(t,0) = \frac{\mu^2}{2}(1 + \sin(3\pi t/T_{max})),$$

where the space interval is $[0,6]$ and the observation time is $T_{max} = 20$, with $\Delta x = 0.1$ and $\Delta t = 0.05$. On each processor $e = 1,2,3,4$ we assume $\mu(0,x) = \mu^e$ and incoming and outgoing boundary data are given by μ^e. Observe that even in this case the inflow profile $\rho^1(t,0)$ exceeds the maximum capacity of the processors.

Referring to Göttlich et al. (2006) we make simulations setting parameters as in Table 2 and we assume to have default processing velocities on each processor, namely $m^e = 1, e = 1,2,3,4$.

In the next Fig. 14 it is depicted the evolution in time of flux, density and processing rate obtained by the Riemann Solver SC1 for $\varepsilon = 0.1$, while in Figg. 15 and 16 we show the behaviour of flux, density and processing rate obtained, respectively, by the Riemann Solvers SC2 and SC3.

Let us make a comparison between graphics in Figg. 14 and 15. We observe that with Solver SC2 the productivity collapses, thus provoking a lowering in the values of the flux and the density. On the other hand, SC1 maintains the level of productivity. Using Solver SC3, which maximizes the flux and adjusts the processing rate if necessary, results are in accordance with those obtained in Göttlich et al. (2006), see Fig. 16.

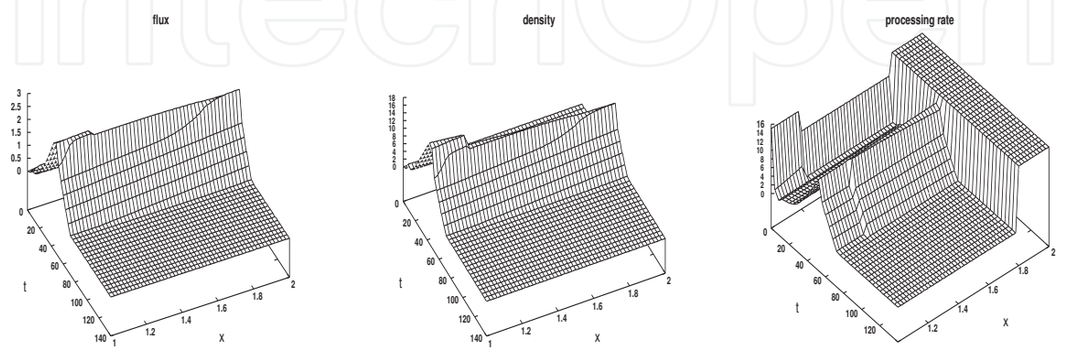

Fig. 10. Test 1: evolution on processors 2, 3, 4, of f (left), ρ (central) and μ (right) using SC2, with data in Table 1 and $\varepsilon = 0.1$.

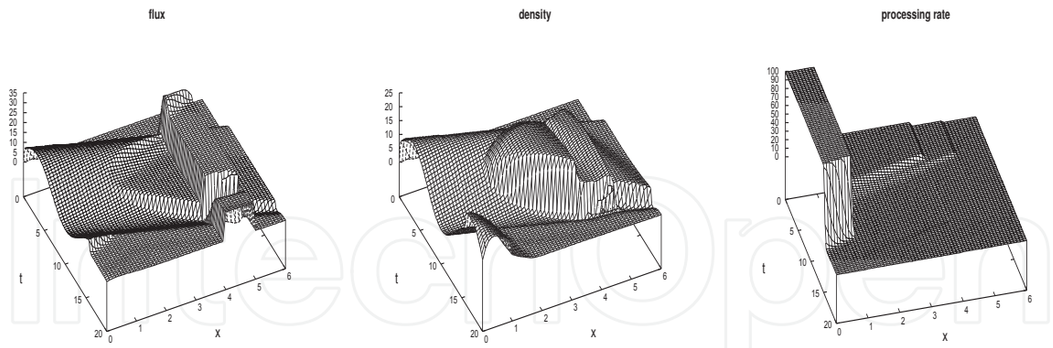

Fig. 11. Test 1: evolution on processors 2, 3, 4, of f (left), ρ (central) and μ (right) using SC3, with data in Table 1 and $\varepsilon = 0.1$.

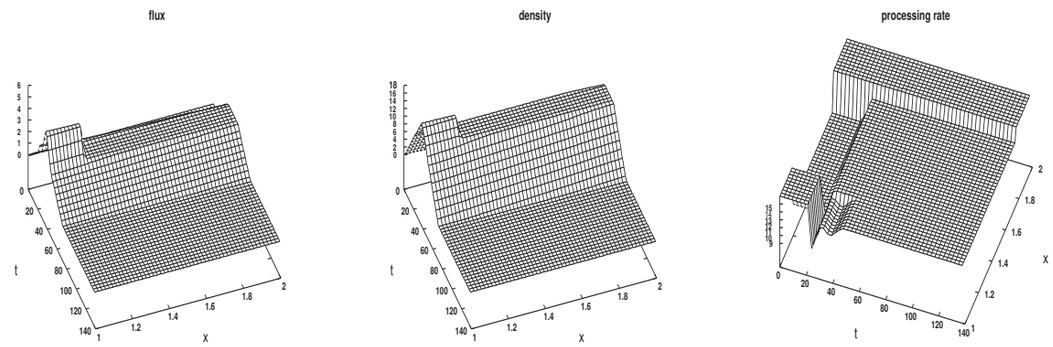

Fig. 12. Test 1: evolution on processors 2, 3, 4, of f (left), ρ (central) and μ (right) using SC3, with data in Table 1 and $\varepsilon = 0.5$.

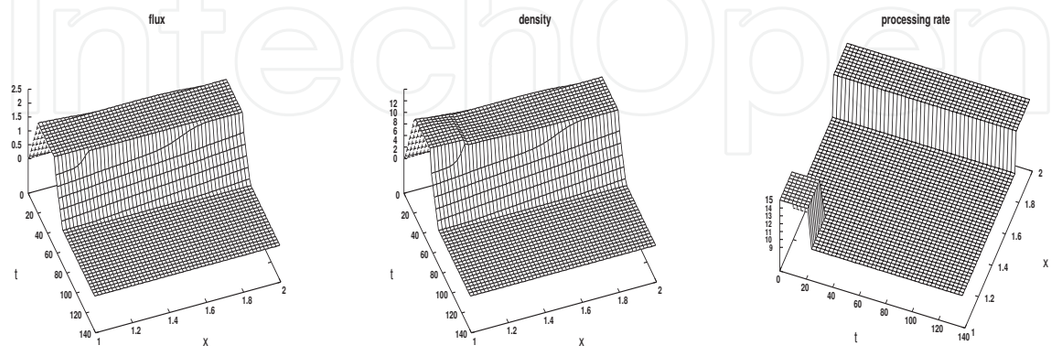

Fig. 13. Test 1: evolution on processors 2, 3, 4, of f (left), ρ (central) and μ (right) using SC3, with data in Table 1 and $\varepsilon = 0.01$.

3. A continuum-discrete model for supply networks

The aim of this Section is to extend the continuum-discrete model regarding sequential supply chains to supply networks which consist of arcs and two types of nodes: nodes with one incoming arc and more outgoing ones and nodes with more incoming arcs and one outgoing arc (see Figure 17). In fact, these two types of nodes are the most common in real supply networks.

3.1 Model description

Let us introduce briefly the model.

Definition 16 *(Network definition) A supply network is a finite, connected directed graph consisting of a finite set of arcs* $\mathcal{A} = \{1, ..., N+1\}$ *and a finite set of junctions* $\mathcal{V}$.

On each arc the load dynamic is given again by a continuum system of type (3). The Riemann Problems at the nodes are solved fixing two "routing" algorithms:

RA1 We assume that

(A) the flow from incoming arcs is distributed on outgoing arcs according to fixed coefficients;

(B) respecting (A) the processor chooses to process goods in order to maximize fluxes (i.e., the number of goods which are processed).

RA2 We assume that the number of goods through the junction is maximized both over incoming and outgoing arcs.

The two algorithms were already used in D'Apice et al. (2006) for the analysis of packets flows in telecommunication networks. Notice that the second algorithm allows the redirection of goods, taking into account possible high loads of outgoing arcs. For both routing algorithms the flux of goods is maximized considering one of the two additional rules, SC2 and SC3.

3.2 Solution of Riemann Problems at nodes

In this Section we discuss Riemann Solvers, which conserve the flux at nodes. We consider two kinds of nodes:

- a node with more incoming arcs and one outgoing one;

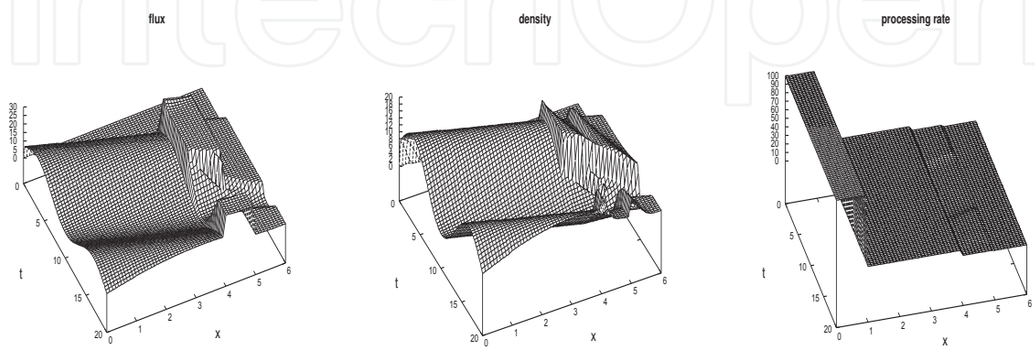

Fig. 14. Test 2: evolution of f (left), ρ (central), μ (right) for the default velocities using SC1, with data in Table 2 and $\varepsilon = 0.1$.

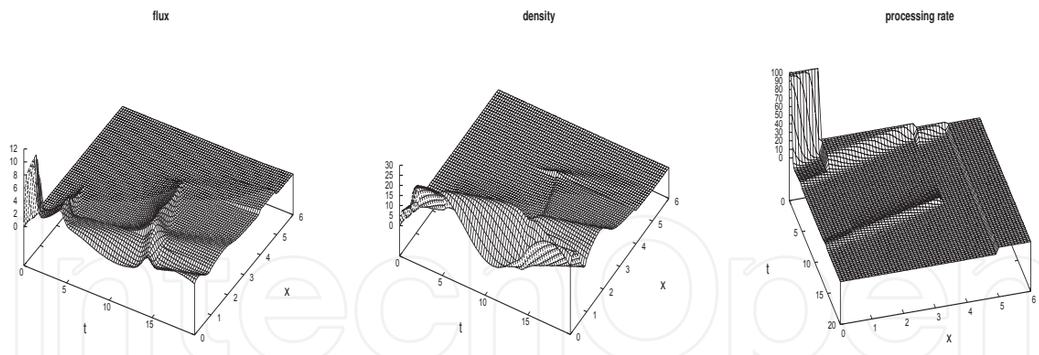

Fig. 15. Test 2: evolution of f (left), ρ (central), μ (right) using SC2, with data in Table 2 and $\varepsilon = 0.1$.

- a node with one incoming arc and more outgoing ones.

We consider a node v^e with n incoming arcs and m outgoing ones and a Riemann initial datum $(\rho^{1,0}, \mu^{1,0}, ..., \rho^{n,0}, \mu^{n,0}, \rho^{n+1,0}, \mu^{n+1,0}, ..., \rho^{n+m,0}, \mu^{n+m,0})$.
The following Lemma holds:

Lemma 17 *On the incoming arcs, only waves of the first family may be produced, while on the outgoing arcs only waves of the second family may be produced.*

From Lemma 17, given the initial datum, for every Riemann Solver it follows that

$$\begin{array}{ll} \hat{\rho}^e = \varphi(\hat{\mu}^e), & e \in \delta_v^-, \\ \hat{\mu}^e = \mu^{e,0}, & e \in \delta_v^+, \end{array} \tag{13}$$

where again $\varphi(\cdot)$ describes the first family curve through $(\rho^{e,0}, \mu^{e,0})$ as function of $\hat{\mu}^e$ and for a fixed vertex v, δ_v^- denotes the sets of ingoing arcs and δ_v^+ the set of outgoing ones.
We define two different Riemann Solvers at a junction that represent the two different routing algorithms RA1 and RA2. For both routing algorithms we can maximize the flux of goods considering one of the two additional rules SC2 and SC3.
To define Riemann Problems according to rule RA1 and RA2 let us introduce the notation:

$$f^e = f(\rho^e, \mu^e).$$

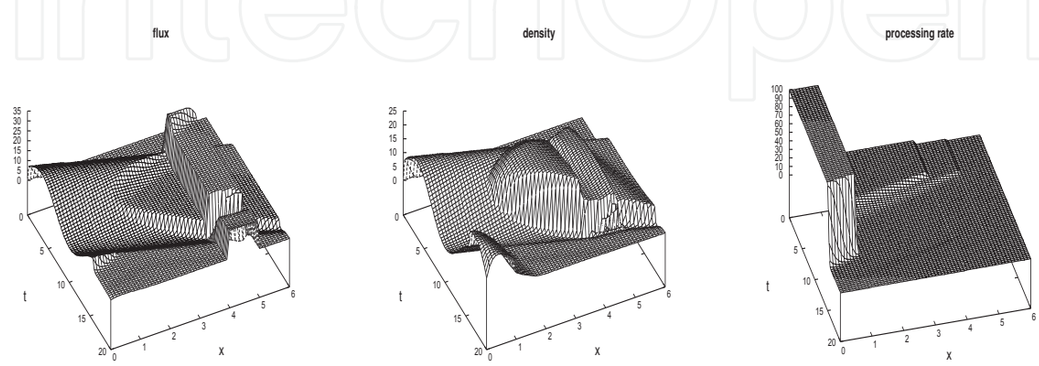

Fig. 16. Test 2: evolution of f (left), ρ (central), μ (right) using SC3, with data in Table 2 and $\varepsilon = 0.1$.

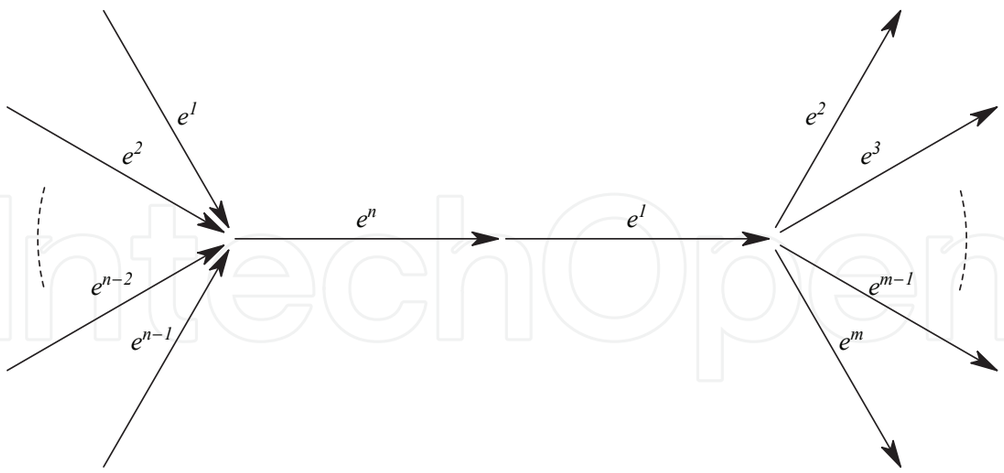

Fig. 17. One outgoing arc (left); one incoming arc (right).

Define the maximum flux that can be obtained by a wave solution on each production arc:

$$f^e_{\max} = \begin{cases} \bar{\mu}^e, & e \in \delta_v^-, \\ \mu^{e,0} + \varepsilon(\rho_M(\mu^{e,0}) - \mu^{e,0}), & e \in \delta_v^+. \end{cases}$$

Since $\hat{f}^e \in [f^e_{\min}, f^e_{\max} = \bar{\mu}^e], e \in \delta_v^-$ and $\hat{f}^e \in [0, f^e_{\max} = \mu^{e,0} + \varepsilon(\rho_M(\mu^{e,0}) - \mu^{e,0})], e \in \delta_v^+$ it follows that if

$$\sum_{e \in \delta_v^-} f^e_{\min} > \sum_{e \in \delta_v^+} f^e_{\max}$$

the Riemann Problem does not admit solution. Thus we get the following condition for the solvability of the supply network.

Lemma 18 *A necessary and sufficient condition for the solvability of the Riemann Problems is that*

$$\sum_{e \in \delta_v^-} f^e_{\min} \leq \sum_{e \in \delta_v^+} \mu^{e,o} + \varepsilon(\rho^M(\mu^{e,o}) - \mu^{e,o}).$$

Lemma 19 *A sufficient condition for the solvability of the Riemann Problems, independent of the initial data, is the following*

$$\sum_{e \in \delta_v^-} \rho^e_{\max} \leq \sum_{e \in \delta_v^+} \mu^e_{\max}.$$

In what follows, first we consider a single junction $v^e \in \mathcal{V}$ with $n-1$ incoming arcs and 1 outgoing arc (shortly, a node of type $(n-1) \times 1$) and then a junction with 1 incoming arc and $m-1$ outgoing ones (shortly, a node of type $1 \times (m-1)$).

3.2.1 One outgoing arc

In this case the two algorithms RA1 and RA2 coincide since there is only one outgoing arc.
We fix a node v^e with $n-1$ incoming arcs and 1 outgoing one and a Riemann initial datum $(\rho^0, \mu^0) = (\rho^{1,0}, \mu^{1,0}, ..., \rho^{n-1,0}, \mu^{n-1,0}, \rho^{n,0}, \mu^{n,0})$. Let us denote with $(\hat{\rho}, \hat{\mu}) =$

$(\hat{\rho}^1,\hat{\mu}^1,...,\hat{\rho}^{n-1},\hat{\mu}^{n-1},\hat{\rho}^n,\hat{\mu}^n)$ the solution of the Riemann Problem. In order to solve the dynamics we have to introduce the priority parameters $(q_1,q_2,...,q_{n-1})$ which determine a *level of priority* at the junction of incoming arcs.
Let us define

$$\Gamma_{inc} = \sum_{i=1}^{n-1} f^i_{\max},$$

$$\Gamma_{out} = f^n_{\max},$$

and $\Gamma = \min\{\Gamma_{inc},\Gamma_{out}\}$.
We analyze for simplicity the case in which $n = 3$, in this case we need only one priority parameter $q \in]0,1[$. Think, for example, of a filling station for soda cans. The arc 3 fills the cans, whereas arcs 1 and 2 produce plastic and aluminium cans, respectively.
First, we compute $\hat{f}^e$ $e = 1,2,3$ and then $\hat{\rho}^e$ and $\hat{\mu}^e, e = 1,2,3$.
We have to distinguish two cases:

Case 1) $\Gamma = \Gamma_{inc}$,

Case 2) $\Gamma < \Gamma_{inc}$.

In the first case we set $\hat{f}^i = f^i_{\max}$, $i = 1,2$. Let us analyze the second case in which we use the priority parameter q.
Not all objects can enter the junction, so let C be the amount of objects that can go through. Then qC objects come from first arc and $(1-q)C$ objects from the second. Consider the space (f^1,f^2) and define the following lines:

$$r_q : f^2 = \frac{1-q}{q} f^1,$$

$$r_\Gamma : f^1 + f^2 = \Gamma.$$

Define P to be the point of intersection of the lines r_q and r_Γ. Recall that the final fluxes should belong to the region (see Fig. 18):

$$\Omega = \left\{ \left(f^1,f^2\right) : 0 \le f^i \le f^i_{\max}, i = 1,2 \right\}.$$

We distinguish two cases:

a) P belongs to Ω,

b) P is outside Ω.

In the first case we set $\left(\hat{f}^1,\hat{f}^2\right) = P$, while in the second case we set $\left(\hat{f}^1,\hat{f}^2\right) = Q$, with $Q = proj_{\Omega\cap r_\Gamma}(P)$ where *proj* is the usual projection on a convex set, see Fig. 18.
Notice that $\hat{f}^3 = \Gamma$.

Remark 20 *The reasoning can be repeated also in the case of $n-1$ incoming arcs. In $\mathbb{R}^{n-1}$ the line r_q is given by $r_q = th_q, t \in \mathbb{R}$, with $h_q \in \Delta_{n-2}$ where*

$$\Delta_{n-2} = \left\{ (f^1,...,f^{n-1}) : f^i \ge 0, i = 1,...,n-1, \sum_{i=1}^{n-1} f^i = 1 \right\}$$

is the $(n-2)$ *dimensional simplex and*

$$H_\Gamma = \left\{ (f^1,...,f^{n-1}) : \sum_{i=1}^{n-1} f^i = \Gamma \right\}$$

is a hyperplane. Since $h_q \in \Delta_{n-2}$*, there exists a unique point* $P = r_q \cap H_\Gamma$*. If* $P \in \Omega$*, then we set* $(\hat{f}^1,...,\hat{f}^{n-1}) = P$*. If* $P \notin \Omega$ *, then we set* $(\hat{f}^1,...,\hat{f}^{n-1}) = Q = proj_{\Omega \cap H_\Gamma}(P)$*, the projection over the subset* $\Omega \cap H_\Gamma$*. Observe that the projection is unique since* $\Omega \cap H_\Gamma$ *is a closed convex subset of* H_Γ*.*

Let us compute $\hat{\rho}^e$ and $\hat{\mu}^e, e = 1,2,3$.
On the incoming arcs we have to distinguish two subcases:

Case 2.1) $\hat{f}^i = f^i_{\max}$. We set according to rules SC2 and SC3,

$$SC2: \begin{array}{l} \hat{\rho}^i = \bar{\mu}^i, \\ \hat{\mu}^i = \bar{\mu}^i, \end{array} \quad i = 1,2,$$

$$SC3: \begin{array}{l} \hat{\rho}^i = \bar{\mu}^i, \\ \hat{\mu}^i = \max\{\bar{\mu}^i, \mu^{i,0}\}, \end{array} \quad i = 1,2.$$

Case 2.2) $\hat{f}^i < f^i_{\max}$. In this case there exists a unique $\hat{\mu}^i$ such that $\hat{\mu}^i + \varepsilon(\varphi(\hat{\mu}^i) - \hat{\mu}^i) = \hat{f}^i$. According to (13), we set $\hat{\rho}^i = \varphi(\hat{\mu}^i), i = 1,2$.

Observe that in case 2.1) $\hat{\rho}^i = \varphi(\hat{\mu}^i) = \bar{\mu}^i, i = 1,2$.
On the outgoing arc we have:

$$\hat{\mu}^3 = \mu^{3,0},$$

while $\hat{\rho}^3$ is the unique value such that $f_\varepsilon(\mu^{3,0}, \hat{\rho}^3) = \hat{f}^3$.

3.2.2 One incoming arc

We fix a node v^e with 1 incoming arc and $m-1$ outgoing ones and a Riemann initial datum $(\rho^0, \mu^0) = (\rho^{1,0}, \mu^{1,0}, \rho^{2,0}, \mu^{2,0}, ..., \rho^{m,0}, \mu^{m,0})$. Let us denote with $(\hat{\rho}, \hat{\mu}) = (\hat{\rho}^1, \hat{\mu}^1, \hat{\rho}^2, \hat{\mu}^2, ..., \hat{\rho}^m, \hat{\mu}^m)$ the solution of the Riemann Problem. Since we have more than one outgoing arc, we need to define the distribution of goods from the incoming arc.

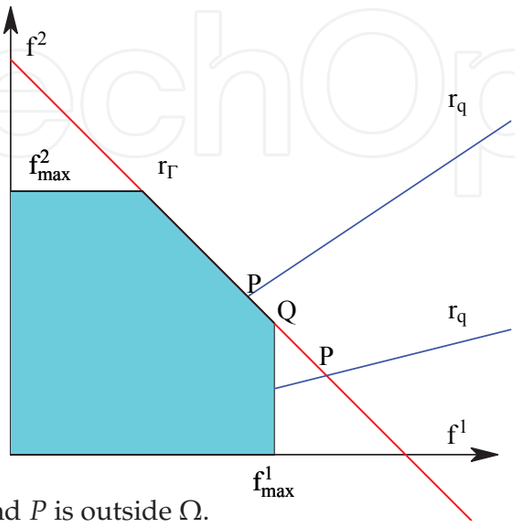

Fig. 18. P belongs to Ω and P is outside Ω.

Introduce the flux distribution parameters α_j, $j = 2,...,m$, where

$$0 < \alpha_j < 1, \sum_{j=2}^{m} \alpha_j = 1.$$

The coefficient α_j denotes the percentage of objects addressed from the arc 1 to the arc j. The flux on the arc j is thus given by

$$f^j = \alpha_j f^1, \; j = 2,...,m,$$

where f^1 is the incoming flux on the arc 1.
Let us define

$$\Gamma_{inc} = f^1_{\max},$$
$$\Gamma_{out} = \sum_{j=2}^{m} f^j_{\max},$$

and $\Gamma = \min\{\Gamma_{inc}, \Gamma_{out}\}$.
We have to determine $\hat{\mu}^e$ and $\hat{\rho}^e, e = 1,...,m$ for both algorithms RA1 and RA2.

3.2.3 Riemann Solver according to RA1.

Analyze the general case with m arcs. Consider, for example, the filling station for fruit juice bottle of Introduction. The arcs e^3 and e^4 fill bottles with pear and apple fruit juices, respectively, according to the bottle shapes. The dynamics at node v^2 is solved using the algorithm we are going to describe. Since $\hat{f}^j \le f^j_{\max}$ it follows that

$$\hat{f}^1 \le \frac{f^j_{\max}}{\alpha_j}, j = 2,...,m.$$

We set

$$\begin{array}{l} \hat{f}^1 = \min\{f^1_{\max}, \frac{f^j_{\max}}{\alpha_j}\}, \quad j = 2,...,m. \\ \hat{f}^j = \alpha_j \hat{f}^1, \end{array}$$

On the incoming arc we have to distinguish two subcases:

Case 1) $\hat{f}^1 = f^1_{\max}$. According to rules SC2 and SC3, respectively, we set

$$SC2: \begin{array}{l} \hat{\rho}^1 = \bar{\mu}^1, \\ \hat{\mu}^1 = \bar{\mu}^1, \end{array}$$

$$SC3: \begin{array}{l} \hat{\rho}^1 = \bar{\mu}^1, \\ \hat{\mu}^1 = \max\{\bar{\mu}^1, \mu^{1,0}\}. \end{array}$$

Case 2) $\hat{f}^1 < f^1_{\max}$. In this case there exists a unique $\hat{\mu}^1$ such that $\hat{\mu}^1 + \varepsilon(\varphi(\hat{\mu}^1) - \hat{\mu}^1) = \hat{f}^1$. According to (13), we set $\hat{\rho}^1 = \varphi(\hat{\mu}^1)$.

On the outgoing arc we have:

$$\hat{\mu}^j = \mu^{j,0}, j = 2,3,$$

while $\hat{\rho}^j$ is the unique value such that $f_\varepsilon(\mu^{j,0}, \hat{\rho}^j) = \hat{f}^j, j = 2,3$.

3.2.4 Riemann Solver according to RA2.

Let us analyze for simplicity the case in which $m = 3$, in this case we need only one distribution parameter $\alpha \in]0,1[$. Think, for example, the supply network of cup production described in the Introduction. The dynamics at the node is solved according to the algorithm RA2. Compute $\hat{f}^e, e = 1,2,3$.
We have to distinguish two cases:

Case 1) $\Gamma = \Gamma_{out}$,

Case 2) $\Gamma < \Gamma_{out}$.

In the first case we set $\hat{f}^j = f^j_{\max}, j = 2,3$. Let us analyze the second case in which we use the priority parameter α.
Not all objects can enter the junction, so let C be the amount of objects that can go through. Then αC objects come from the first arc and $(1-\alpha)C$ objects from the second. Consider the space (f^2, f^3) and define the following lines:

$$r_\alpha : f^3 = \frac{1-\alpha}{\alpha} f^2,$$

$$r_\Gamma : f^2 + f^3 = \Gamma.$$

Define P to be the point of intersection of the lines r_α and r_Γ. Recall that the final fluxes should belong to the region:

$$\Omega = \left\{ \left(f^2, f^3\right) : 0 \le f^j \le f^j_{\max}, j = 2,3 \right\}.$$

We distinguish two cases:

a) P belongs to Ω,

b) P is outside Ω.

In the first case we set $\left(\hat{f}^2, \hat{f}^3\right) = P$, while in the second case we set $\left(\hat{f}^2, \hat{f}^3\right) = Q$, with $Q = proj_{\Omega \cap r_\Gamma}(P)$ where $proj$ is the usual projection on a convex set. Observe that $\hat{f}^1 = \Gamma$.
Again, we can extend the reasoning to the case of $m-1$ outgoing arcs as for the incoming arcs defining the hyperplane

$$H_\Gamma = \left\{ (f^2, ..., f^m) : \sum_{j=2}^{m} f^j = \Gamma \right\}$$

and choosing a vector $h_\alpha \in \Delta_{m-2}$. Moreover, we compute $\hat{\rho}^e$ and $\hat{\mu}^e$ in the same way described for the Riemann Solver RA1.

3.3 Numerical experiments

In what follows we report the densities and production rates at the instant $t = 0$ and after some times (at $t = 1$) for different initial data using different routing algorithms. Since a constant state is an equilibrium for the single line model, a modification of the state may only appear initially at the junction. In Table 3 and in Fig. 19-20 we report the Riemann Solver for a node of type 1×2 and assume $\varepsilon = 0.2, \mu^e_{\max} = 1, e = 1,2,3, \alpha = 0.8, (\rho^{1,0}, \rho^{2,0}, \rho^{3,0}) = (0.7,0.1,0), (\mu^{1,0}, \mu^{2,0}, \mu^{3,0}) = (1,0.2,1)$. Observe that the algorithm RA2 redirects the goods, in fact taking into account the initial loads of the outgoing sub-chains, the number of goods processed by the sub-chain with density $\rho^{3,0} = 0$ increases.
In Table 4 and in Figg. 21-22 we report numerical results for a node of type 2×1, and assume $\varepsilon = 0.2, \mu^e_{\max} = 1, e = 1,2,3, q = 0.6, (\rho^{1,0}, \rho^{2,0}, \rho^{3,0}) = (0.3,0.7,0.8)$, $(\mu^{1,0}, \mu^{2,0}, \mu^{3,0}) = (0.8,0.7,0.4)$.

	RA1		RA2	
	SC2	SC3	SC2	SC3
$\hat{f}^e$	$(0.58, 0.47, 0.12)$	$(0.58, 0.47, 0.12)$	$(0.7, 0.47, 0.23)$	$(0.7, 0.47, 0.23)$
$\hat{\rho}^e$	$(0.82, 1.53, 0.12)$	$(0.82, 1.53, 0.12)$	$(0.7, 1.53, 0.23)$	$(0.7, 1.53, 0.23)$
$\hat{\mu}^e$	$(0.52, 0.2, 1)$	$(0.52, 0.2, 1)$	$(0.7, 0.2, 1)$	$(1, 0.2, 1)$

Table 3. A node of type 1×2.

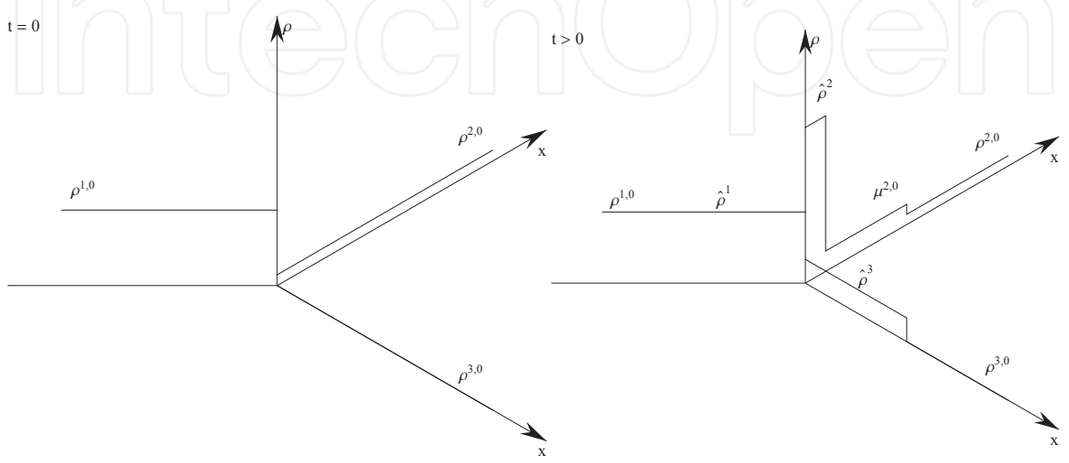

Fig. 19. A RP for the RA2-SC3 algorithm: the initial density and the density after some times.

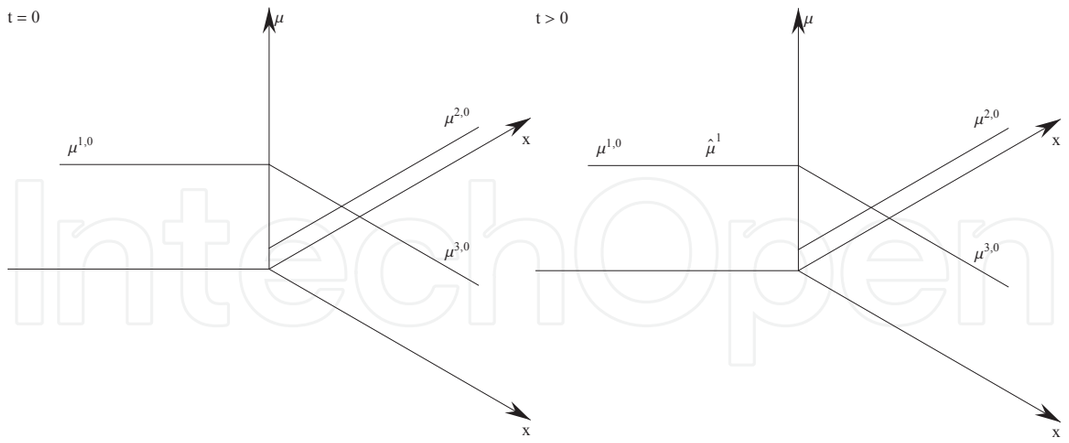

Fig. 20. A RP for the RA2-SC3 algorithm: the initial production rate and the production rate after some times.

	RA1=RA2	
	SC2	SC3
$\hat{f}^e$	$(0.3, 0.3, 0.6)$	$(0.3, 0.3, 0.6)$
$\hat{\rho}^e$	$(0.3, 1.1, 1.4)$	$(0.3, 1.1, 1.4)$
$\hat{\mu}^e$	$(0.3, 0.1, 0.4)$	$(0.8, 0.1, 0.4)$

Table 4. A node of type 2×1.

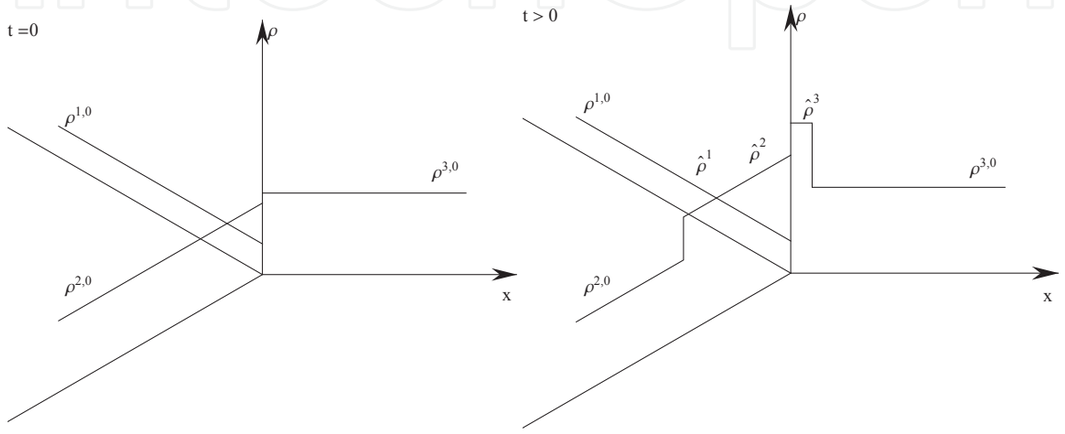

Fig. 21. A RP for the SC2 algorithm: the initial density and the density after some times.

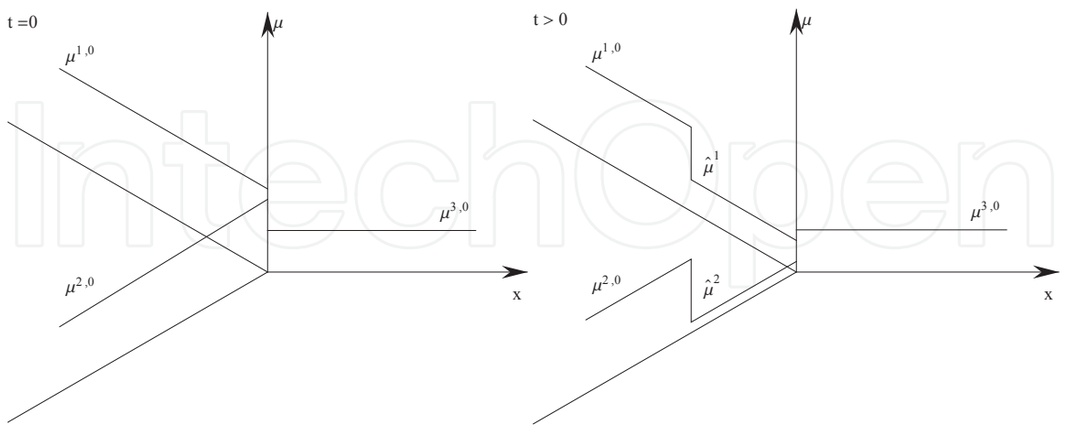

Fig. 22. A RP for the SC2 algorithm: the initial production rate and the production rate after some times.

4. Conclusions

In this Chapter we have proposed a mixed continuum-discrete model, i.e. the supply chain is described by continuous arcs and discrete nodes, it means that the load dynamics is solved in a continuous way on the arcs, and at the nodes imposing conservation of goods density, but not of the processing rate. In fact, each arc is modelled by a system of two equations: a conservation law for the goods density, and an evolution equation for the processing rate. The mixed continuum-discrete model is useful when there is the possibility to reorganize the supply chain: in particular, the productive capacity can be readapted for some contingent necessity. Possible choices of solutions at nodes guaranteeing the conservation of fluxes are analyzed. In particular Riemann Solvers are defined fixing the rules SC1, SC2, SC3. The numerical experiments show that SC1 appears to be very conservative (as expected), while SC2 and SC3 are more elastic, thus allowing more rich dynamics. Then, the main difference between SC2 and SC3 is the following. SC2 tends to make adjustments of the processing rate more than SC3, even when it is not necessary for purpose of flux maximization. Thus, when oscillating waves reach an arc, then SC2 reacts by cutting such oscillations. In conclusion, SC3 is more appropriate to reproduce also the well known "bull-whip" effect. The continuum-discrete model, regarding sequential supply chains, has been extended to supply networks with nodes of type $1 \times n$ and $m \times 1$. The Riemann Problems are solved fixing two "routing" algorithms RA1 and RA2, already used for the analysis of packets flows in telecommunication networks. For both routing algorithms the flux of goods is maximized considering one of the two additional rules, SC2 and SC3.
In future we aim to develop efficient numerics for the optimal configuration of a supply chain, in particular of the processing rates, facing the problem to adjust the production according to the supply demand in order to obtain an expected pre-assigned outflow.

5. References

Armbruster, D.; De Beer, C.; Freitag, M.; Jagalski, T.; Ringhofer, C. & Rascle, M. (2006). Autonomous Control of Production Networks using a Pheromone Approach, *Physica A: Statistical Mechanics and its applications*, Vol. 363, Issue 1, pp. 916-938.

Armbruster, D.; Degond, P. & Ringhofer, C. (2006). A model for the dynamics of large queuing networks and supply chains, *SIAM Journal on Applied Mathematics*, Vol. 66, Issue 3, pp. 896-920.

Armbruster, D.; Degond, P. & Ringhofer, C. (2006). Kinetic and fluid Models for supply chains supporting policy attributes, *Transportation Theory Statist. Phys.*

Armbruster, D.; Marthaler, D. & Ringhofer, C. (2004). Kinetic and fluid model hierarchies for supply chains, *SIAM J. on Multiscale Modeling*, Vol. 2, No. 1, pp. 43-61.

Bressan, A. (2000). *Hyperbolic Systems of Conservation Laws - The One-dimensional Cauchy Problem*, Oxford Univ. Press.

Bretti, G.; D'Apice, C.; Manzo, R. & Piccoli, B. (2007). A continuum-discrete model for supply chains dynamics, *Networks and Heterogeneous Media*, Vol. 2, No. 4, pp. 661-694.

Daganzo, C.F. (2003). *A theory of supply chains*, Lecture Notes in Economics and Mathematical Systems. 526. Berlin: Springer. viii, 123 p.

D'Apice, C. & Manzo, R. (2006). A fluid-dynamic model for supply chain, *Networks and Heterogeneous Media*, Vol. 1, No. 3, pp. 379-389.

D'Apice, C.; Manzo, R. & Piccoli, B. (2006). Packet flow on telecommunication networks, *SIAM J. Math. Anal.*, Vol. 38, No. 3, pp. 717-740.

D'Apice, C.; Manzo, R. & Piccoli, B. (2009). Modelling supply networks with partial differential equations, *Quarterly of Applied Mathematics*, Vol. 67, No. 3, pp. 419-440.

D'Apice, C.; Manzo, R. & Piccoli, B. (2010). Existence of solutions to Cauchy problems for a mixed continuum-discrete model for supply chains and networks, *Journal of Mathematical Analysis and Applications*, Vol. 362, No. 2, pp. 374-386.

Göttlich, S.; Herty, M. & Klar, A. (2005). Network models for supply chains, *Comm. Math. Sci.*, Vol. 3, No. 4, pp. 545-559.

Göttlich, S.; Herty, M. & Klar, A. (2006). Modelling and optimization of Supply Chains on Complex Networks, *Comm. Math. Sci.*, Vol. 4, No. 2, pp. 315-330.

Helbing D.; Armbruste D. ; Mikhailov A. & Lefeber E (2006). Information and material flows in complex networks, *Phys. A*, Vol. 363, pp. xi–xvi.

Helbing, D.; Lämmer, S.; Seidel, T.; Seba, P. & Platkowski, T. (2004). Physics, stability and dynamics of supply networks, *Physical Review E*, Vol. 3, 066116.

Helbing, D. & Lämmer, S. (2005). Supply and production networks: From the bullwhip effect to business cycles, *Armbruster, D.; Mikhailov A. S.; & Kaneko; K. (eds.) Networks of Interacting Machines: Production Organization in Complex Industrial Systems and Biological Cells, World Scientific, Singapore*, pp. 33–66.

Herty, M.; Klar, A. & Piccoli, B. (2007). Existence of solutions for supply chain models based on partial differential equations, *SIAM J. Math. Anal.*, Vol. 39, No. 1, pp. 160-173.

Nagatani, T. & Helbing, D. (2004). Stability analysis and stabilization strategies for linear supply chains, *Physica A: Statistical and Theoretical Physics*, Vol. 335, Issues 3-4, pp. 644-660.

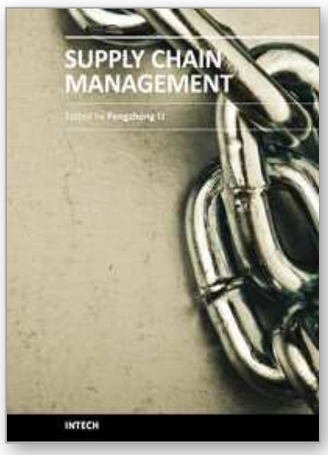

Supply Chain Management
Edited by Dr. pengzhong Li

ISBN 978-953-307-184-8
Hard cover, 590 pages
Publisher InTech
Published online 26, April, 2011
Published in print edition April, 2011

The purpose of supply chain management is to make production system manage production process, improve customer satisfaction and reduce total work cost. With indubitable significance, supply chain management attracts extensive attention from businesses and academic scholars. Many important research findings and results had been achieved. Research work of supply chain management involves all activities and processes including planning, coordination, operation, control and optimization of the whole supply chain system. This book presents a collection of recent contributions of new methods and innovative ideas from the worldwide researchers. It is aimed at providing a helpful reference of new ideas, original results and practical experiences regarding this highly up-to-date field for researchers, scientists, engineers and students interested in supply chain management.

How to reference
In order to correctly reference this scholarly work, feel free to copy and paste the following:

Ciro D'Apice, Rosanna Manzo and Benedetto Piccoli (2011). Continuum-Discrete Models for Supply Chains and Networks, Supply Chain Management, Dr. pengzhong Li (Ed.), ISBN: 978-953-307-184-8, InTech, Available from: http://www.intechopen.com/books/supply-chain-management/continuum-discrete-models-for-supply-chains-and-networks

INTECH
open science | open minds

InTech Europe
University Campus STeP Ri
Slavka Krautzeka 83/A
51000 Rijeka, Croatia
Phone: +385 (51) 770 447
Fax: +385 (51) 686 166
www.intechopen.com

InTech China
Unit 405, Office Block, Hotel Equatorial Shanghai
No.65, Yan An Road (West), Shanghai, 200040, China
中国上海市延安西路65号上海国际贵都大饭店办公楼405单元
Phone: +86-21-62489820
Fax: +86-21-62489821

IntechOpen